A Unified Parametric Representation for Robotic Compliant Skills with Adaptation of Impedance and Force

Chao Zeng, *Member*, *IEEE*, Yanan Li, *Senior Member*, *IEEE*, Jing Guo, Zhifeng Huang, *Member*, *IEEE*, Ning Wang, Chenguang Yang, *Senior Member*, *IEEE*

***Abstract*—Robotic compliant manipulation is a very challenging but urgent research spot in the domain of robotics. One difficulty lies in the lack of a unified representation for encoding and learning of compliant profiles. This work aims to introduce a novel learning and control framework to address this problem: i) we provide a parametric representation that enables a compliant skill to be encoded in a parametric space and allows a robot to learn compliant manipulation skills based on motion and force information collected from human demonstrations; and ii) the updating laws of the compliant profiles including impedance and force profiles are derived from a biomimetic control strategy based on the human motor learning principles. Our approach enables the simultaneous adaptation of impedance and feedforward force online during robot's reproduction of the demonstrated tasks to deal with task dynamics and external interferences. The proposed approach is verified based on both simulation and real-world task scenarios.**

***Index Terms*—Impedance and force learning; biomimetic control; Compliant manipulation; Learning from human demonstrations; Human-robot physical interaction.**

I. Introduction

Learning manipulation skills from humans can enable a robot to effectively acquire the ability to perform particular tasks [1], just requiring a limited number of demonstrations. It has recently become a research hot spot in the relevant field because of a number of advantages. The most important one is probably that it has a big potential to bring human factors into robotic systems, and therefore to combine the advantages of both humans and robots. Learning from human demonstration (LfHD) has been proven to be one promising way for robots to learn different types of tasks, including industrial assembly [2], surgical manipulation [3], and autonomous navigation [4], etc.

Despite many exciting examples and improvements in robot learning, so far learning compliant manipulation is still an open challenging problem. Only learning of motion primitives/features is usually not enough to encode a skill when it comes to the term of compliance. More features such as impedance and force need to be considered and included in the skill-encoding process [5–7]. In a common grasping task, for instance, we should not only consider where to grasp but also need to know how much force is needed for grasping different objects with rigid or soft characteristics. In this sense, how to adapt the impedance/force profiles in a specific task needs to be addressed. In other words, how impedance/force profiles should respond to task dynamics with respect to the evolution of motion trajectories needs to be answered. In this paper, we propose a novel mechanism for adaptation of impedance and force profiles which is inspired by a biomimetic control strategy developed from human motor learning regulations in the muscle space. In order to overcome uncertainties caused by environmental interferences, these profiles are learned and adapted online automatically during the task reproduction based on the prior knowledge of motion and force information collected from demonstrations.

In this work, we propose a unified representation framework for the encoding of compliant skills. Several learning and control approaches have been developed so far for robot compliant manipulation. However, most of these are focused on either learning or control, namely, learning and control are treated separately. Inspired by human motor learning, we argue that they can be integrated in a unified manner. Furthermore, in the domain of robot control it has illustrated that learning algorithms can be used for control (see, e.g., [5, 8, 9]), i.e., *learning for control*. In contrast, this paper argues that it is also reasonable to implement control strategies for learning robotic skills, i.e., *control for learning*.

We seek to provide a representation of the compliant profiles. If we want manipulation skills to be shared and transferred across different robot platforms and task scenarios in the future, it would be better to represent them in a unified way [10]. In this work, we propose to convert the compliant profiles including motion trajectories, impedance, and force profiles from trajectory-level into a parametric space. And the adaptation of these trajectories is achieved directly in the parametric space instead of trajectory-level updating. One advantage of doing this is that we can use a particular set of parameters to represent a specific skill.

The remainder of this paper is organized as follows: Section II summarizes the most related previous works on this

This work was in part supported by National Nature Science Foundation (NSFC) under Grants 62003096, 51605098, and 61803103, in part by the Fellowship of the China Postdoctoral Science Foundation under Grant 2020M682613, and in part by the Open Fund Project of Fujian Provincial Key Laboratory of Information Processing and Intelligent Control (Minjiang University) under Grant MJUKF-IPIC202003. *(Corresponding authors: J. Guo and C. Yang).*

C. Zeng, J. Guo and Z. Huang are with School of Automation, Guangdong University of Technology, China. {auczeng; jing.guo; zhifeng}@gdut.edu.cn. Y. Li is with the Department of Engineering and Design, University of Sussex, U.K. yl557@sussex.ac.uk. N. Wang and C. Yang are with Bristol Robotics Laboratory, University of the West of England, UK. Katie.Wang@brl.ac.uk; cyang@ieee.org.

topic. Section III reviews the biomimetic control strategy. The proposed approach is detailed in Section IV, followed by the experiments in Section V. Section VI finally concludes this paper and gives possible future research directions.

II. Related works

Trajectory-based movement encoding is an efficient way for robots to imitate, and even generalize human skills. In the last two decades, several types of models have been developed to encode data collected from human demonstrations, to learn motion control strategies from these data, and then to generate control commands based on the learned strategies for robots to reproduce tasks. Among these models, dynamical movement primitives (DMPs) have been widely used in a large number of robotic tasks, thanks to their fine characteristics such as the high-computing efficiency and the good generalizability [11]. DMPs model represents a trajectory by a linear term, plus a non-linear one represented by an inner product of weights and Gaussian basis. Inspired by this, our approach takes a similar but a bit different way, in order to represent the compliant profiles in the parametric space.

Adaptive learning approaches can be utilized for the estimation of a proper impedance profile in an impedance-based torque controller to achieve compliant robotic behaviors [12–15]. They usually enable a robot to follow planned trajectories during which impedance is adapted to meet some specific requirements. However, these approaches may be difficult for learning control commands from demonstration data because the physical interaction force/torque information between the human tutor and the robot needs to be included in the learning process. Reinforcement learning techniques have also been used for adaptive impedance control in robotic manipulation and grasping tasks [16–18]. In this case, it often requires a number of trials with a task-specific cost function to finally obtain a proper impedance profile.

Learning impedance or force/torque primitives has been recently proposed to encode impedance or force/torque data collected from physical demonstrations [19–21]. This approach usually treats the impedance or force/torque similar to the motion trajectories, encoded either by the *non-linear term* stated above [22] or by probabilistic models [23]. This approach has shown good results to deal with LfHD-based physical interaction tasks (see e.g., [22]). However, impedance and force/torque profiles are considered in a separate manner. Until now, there lacks a unified framework to encode all the compliant profiles simultaneously.

To seek solutions for addressing problems in robot compliant manipulation from human motor learning has shown promising performances [24]. Recent findings in neuroscience have revealed that humans can perform task compliantly by properly adapting arm impedance and force following particular principles in the muscle space, under the control of the central nervous systems [25, 26]. Based on these principles, a biomimetic control strategy has been developed in our previous works [27–29] for achieving the robotic compliant behaviors. In this work, we take one step forward to enable this control strategy facilitating robot learning from demonstrations. Further, in order to fit it into the aforementioned unified representation, we enable the updating of the compliant profiles in the parametric space.

To summarize, the novelties and contributions of this work are as follows:

i) We present a LfHD approach derived from a control strategy based on the human motor learning regulations, to address the learning of compliant manipulation skills. The results show that human-inspired control could be promising for robot learning of manipulation skills.

and ii) We provide a unified representation for the encoding of the compliant profiles. The impedance and force profiles can be adapted online during the task reproduction phase, along with the execution of motion trajectories. Further, we propose to encode all the compliant profiles in the parametric space instead of a trajectory-level way.

III. Preliminary

In this section, we briefly review the biomimetic control strategy in [27, 28], which is developed from the human motor learning control.

A. *Robotic impedance controller in Cartesian space*

We consider a rigid-body robot with the dynamics in the Cartesian space as below.

$$M(q)\ddot{x} + C(q,\dot{q})\dot{x} + G(q) = \tau_c + f_{ext} \tag{1}$$

where q is the joint angle, and $\dot{q}$ and $\ddot{q}$ are corresponding joint velocity and acceleration, respectively. x represents the position of the robotic arm endpoint. $M(q)$, $C(q,\dot{q})$ and $G(q)$ represent inertia, Coriolis and centrifugal matrix, and gravitational force, respectively. τ_c is the control input, and f_{ext} represents the external force exerted on the robot by its environment or a human user.

According to the biomimetic control strategy [28], the control input is split into two parts, i.e.,

$$\tau_c = v + w \tag{2}$$

where v is designed to track the reference trajectory x_r by compensating for the robot's dynamics.

$$v = M(q)\ddot{x} + C(q,\dot{q})\dot{x} + G(q) - \Gamma\varepsilon \tag{3}$$

with

$$\dot{x}_e = \dot{x}_r - \alpha e, \quad e = x - x_r \tag{4}$$

where α is a positive constant coefficient. $\dot{x}_e$ is an auxiliary variable defined with the trajectory tracking error e. Γ is a positive-definite matrix, and ε is the sliding operation.

$$\varepsilon = \dot{e} + \alpha e \tag{5}$$

Another term in the controller, i.e., w is designed to compensate for the dynamics during interaction with the external environment, defined by

$$w = -F - K_S x - K_D \dot{x} \tag{6}$$

where F, K_S and K_D represent feedforward force, stiffness and damping, respectively, that are used to compensate for the

counterparts of the environment, with the following assumption.

$$f_{ext} = F^* + K_S^* x + K_D^* \dot{x} \tag{7}$$

where F^*, K_S^* and K_D^* are unknown environmental parameters

B. Adaptation of impedance and feedforward force based on human motor control

According to the computational model of human motor learning [27, 30], the adaptation of impedance and feedforward force can be achieved by concurrently minimizing the cost function as below:

$$J = J_e + J_c \tag{8}$$

where $J_e(t)$ deals with trajectory tracking:

$$J_e(t) = \frac{1}{2}\varepsilon(t)^T M(q)\varepsilon(t) \tag{9}$$

The second term in the cost function, J_c is used to represent the residual errors of feedforward force, stiffness and damping, between the control inputs and the dynamics of the environment, defined by:

$$\begin{aligned} J_c(t) = \frac{1}{2}\int_{t-T}^{t} & [(F^* - F)^T Q_F^{-1}(F^* - F) \\ & + \mathrm{vec}^T(K_S^* - K_S)Q_S^{-1}\mathrm{vec}(K_S^* - K_S) \\ & + \mathrm{vec}^T(K_D^* - K_D)Q_D^{-1}\mathrm{vec}(K_D^* - K_D)]d\tau \end{aligned} \tag{10}$$

with the symmetric positive-definite matrices Q_F, Q_K and Q_D. vec represents the operator for column vectorization.

The minimization of the cost can be achieved through the update laws as below:

$$\Delta K_S(t) = Q_S[\varepsilon(t)x(t)^T - \beta K_S(t)] \tag{11}$$

$$\Delta K_D(t) = Q_D[\varepsilon(t)\dot{x}(t)^T - \beta K_D(t)] \tag{12}$$

$$\Delta F(t) = Q_F[\varepsilon(t) - \beta F(t)] \tag{13}$$

where β is a positive coefficient.

C. Adaptation of reference trajectory for consideration of contact force

This subsection is to introduce how to further adapt the reference trajectory to consider the contact forces between the robot and the environment during the execution of a task, inspired by the fact that humans can do so for adaptation to different environments [31]. As suggested in [28], a desired x_d is assumed to generate the desired contact force, with the same format as in (7), i.e.,

$$F_d = F^* + K_S^* x_d + K_D^* \dot{x}_d \tag{14}$$

Then, the following update law of the reference trajectory x_r is designed to track the desired trajectory x_d by minimizing the error between the control force and the desired force, and it is defined by:

$$\Delta\xi_r(t) = Q_r[F_d(t) - F(t) - \xi_r(t)] \tag{15}$$

where Q_r is also a positive-definite constant matrix set in advance. The auxiliary variable ξ_r is defined as below:

$$\xi_r = K_S x_r + K_D \dot{x}_r \tag{16}$$

Similar to (10), this update law is used for the minimization of the following cost:

$$J_r = \frac{1}{2}\int_{t-T}^{t} (\xi_r - \xi_d)^T Q_r^T (\xi_r - \xi_d)d\tau \tag{17}$$

Then, the adaptation of trajectory Δx_r is achieved by

$$\Delta x_r(t) = K_S^{-1}[\Delta\xi_r(t) - \Delta K_S x_r(t) - \Delta K_D \dot{x}_r(t)] \tag{18}$$

Finally, to couple together the adaptation of the feedforward force and the trajectory, the updating law for the force (13) is modified as:

$$\Delta F(t) = Q_F[\varepsilon(t) - \beta F(t) + Q_r^T \Delta\xi_r(t)] \tag{19}$$

IV. Proposed Approach

In this section, we will first introduce the representation of a compliant skill in the parametric space. Then, we will present how to encode reference trajectories and desired force profiles from human demonstrations. Subsequently, the online learning of impedance and feedforward force in the parametric space will be derived based on the preliminary works. Finally, we will show how to integrate the learning/representation of all these profiles. Some important aspects of the proposed approach will also be briefly commented.

A. Parametric representation of a compliant skill

A compliant skill here is defined as a combination of the reference motion trajectories and the control variables (including impedance, damping, and feedforward force), plus the desired contact force profiles, i.e.,

$$C(t) = [x_r(t), K_S(t), K_D(t), F(t), F_d(t)] \tag{20}$$

where

$$\begin{aligned} x_r(t) &= [x_{r,1}(t), x_{r,2}(t), ..., x_{r,M}(t)]^T \\ K_S(t) &= [K_{S,1}(t), K_{S,2}(t), ..., K_{S,M}(t)]^T \\ K_D(t) &= [K_{D,1}(t), K_{D,2}(t), ..., K_{D,M}(t)]^T \\ F(t) &= [F_1(t), F_2(t), ..., F_M(t)]^T \\ F_d(t) &= [F_{d,1}(t), F_{d,2}(t), ..., F_{d,M}(t)]^T \end{aligned} \tag{21}$$

where M is the number of DOFs (degrees of freedom) of the control space, and the time step $t = 1, 2, ..., T$.

We go further to utilize a set of parameters for the representation of a compliant skill by representing the above trajectories/profiles in a parametric space as follows.

$$\theta(t) = \{\theta_{p,i}(t), \theta_{K_S,i}(t), \theta_{K_D,i}(t), \theta_{F,i}(t), \theta_{F_d,i}(t)\}_{i=1}^{M} \tag{22}$$

where

$$\begin{aligned} \theta_{p,i}(t) &= [\theta_{p,i,1}(t), \theta_{p,i,2}(t), ..., \theta_{p,i,N_p}(t)]^T \\ \theta_{K_S,i}(t) &= [\theta_{K_S,i,1}(t), \theta_{K_S,i,2}(t), ..., \theta_{K_S,i,N_{KS}}(t)]^T \\ \theta_{K_D,i}(t) &= [\theta_{K_D,i,1}(t), \theta_{K_D,i,2}(t), ..., \theta_{K_D,i,N_{KD}}(t)]^T \\ \theta_{F,i}(t) &= [\theta_{F,i,1}(t), \theta_{F,i,2}(t), ..., \theta_{F,i,N_F}(t)]^T \\ \theta_{F_d,i}(t) &= [\theta_{F_d,i,1}(t), \theta_{F_d,i,2}(t), ..., \theta_{F_d,i,N_{FD}}(t)]^T \end{aligned} \tag{23}$$

where $N_{()}$ represents the number of the elements of each corresponding vector.

Compared with the trajectory-level representation, the parametric representation of a compliant skill has several advantages. For instance, optimization techniques may be used to refine the compliant skill through optimizing the parameters, instead of the whole trajectory. Here, the parametric representations $\theta_{p,i}$ and $\theta_{F_d,i}$ for the position trajectories and force profiles are estimated from the data collected from human demonstrations. The other parametric vectors are learned based on the above-mentioned biomimetic control. In the following subsections, we will introduce how to update these parameters in detail.

B. *Learning of reference trajectories and estimation of the desired force from human demonstrations*

1) Learning of reference trajectories: During each human demonstration, the robot states (e.g., endpoint's pose) and the interaction force are recorded. First, we use the well-known DMPs model to encode the motion trajectories. For 1-DOF motion trajectory $x(t)$, the following set of equations are used to encode it by using a parametric representation [32].

$$\tau \dot{z} = \alpha(\beta(x_{goal} - x) - z) + f(s) \tag{24}$$

$$\tau \dot{x} = z \tag{25}$$

$$\tau \dot{s} = -\alpha_s s \tag{26}$$

$$f(s) = \theta_p^T g_p \tag{27}$$

with

$$[g_p]_n = \frac{\omega_n(s)s}{\sum_{n=1}^{N_p} \omega_n(s)}(x_{goal} - x_0) \tag{28}$$

and

$$\omega_n(s) = \exp(-0.5h_n(s - c_n)^2) \tag{29}$$

where x_{goal} is the goal of the trajectory, and x_0 the start point, i.e., $x_0 = x(0)$ and $x_{goal} = x(T)$. $\tau > 0$ is a time scaling factor, $\alpha > 0$, $\beta > 0$, and $\alpha_s > 0$ are constant coefficients. $s \in [0, 1]$ is a phase variable. Note that in (31) θ_p is the parametric vector as defined in (23). Correspondingly, g_p is a basis vector, and the n-th element is defined in (28). Combining with (29), g_p can be regarded as a scaled Gaussian basis vector. N_p is the number of the Gaussian functions, and c_n and h_n are the center and width respectively.

The target is given by

$$\theta_p^T g_p = \tau^2 \ddot{x} + \alpha\tau\dot{x} - \alpha\beta(x_{goal} - x) \tag{30}$$

Then, the parameter θ_p can be estimated by optimizing the target using LWR, given the observation data x.

2) Learning of force profiles: For the desired force F_d, i.e., the measured force data collected from human demonstrations, we use the following equations to convert it into a parametric space.

$$F_d = \theta_{F_d}^T g \tag{31}$$

with

$$[g]_n = \frac{\omega_n(s)}{\sum_{n=1}^{N} \omega_n(s)} \tag{32}$$

The estimation of the parametric vector θ_{F_d} can be achieved similarly using the above recursive regression algorithm by:

$$\min \parallel F_{mes} - \theta_{F_d}^T g \parallel^2 \tag{33}$$

where F_{mes} represents the measured forces during the human demonstration.

C. *Learning of the parameters for the impedance and feedforward force profiles*

1) Representation of the impedance and feedforward force profiles in parametric spaces: We first need to represent the impedance (stiffness and damping) and feedforward force profiles in the parametric spaces, as stated above, to represent all the control variables in a unified manner.

Similarly, they can be represented as a dot product of two vectors, i.e.,

$$K_S = diag\{\theta_{K_S}^T g\}; K_D = diag\{\theta_{K_D}^T g\}; F = \theta_F^T g \tag{34}$$

where g is the Gaussian basis vector which is directly fused from (32). Note that the number of Gaussian functions, i.e., N can be set as different values for different variables here.

2) Adaptation of the impedance and feedforward force: As mentioned above, the impedance and feedforward force are adapted to minimize the tracking error. Here, we propose to adapt them in the parametric spaces, namely, the vectors θ_{K_S}, θ_{K_D} and θ_F are adapted at each time step during a control loop.

According to (11) and (12), we develop the following updating laws for θ_{K_S}, θ_{K_D} and θ_F.

For the m-th DOF at the time step t, they are recursively updated as

$$\theta_{K_S,m,n}(t+1) = \frac{\Omega_1(t) - \sum_{j=1}^{N} \theta_{K_s,m,j,j\neq n}(t) g_{j,j\neq n}}{1 - \sum_{j=1}^{N} g_{j,j\neq n}} \tag{35}$$

with

$$\Omega_1(t) = Q_{K,m}\varepsilon_m(t)x_m(t) + (1 - Q_{K,m}\beta)\theta_{K_S,m}^T(t)g \tag{36}$$

And

$$\theta_{K_D,m,n}(t+1) = \frac{\Omega_2(t) - \sum_{j=1}^{N} \theta_{K_D,m,j,j\neq n}(t) g_{j,j\neq n}}{1 - \sum_{j=1}^{N} g_{j,j\neq n}} \tag{37}$$

Algorithm 1: Online learning of impedance and feedforward force parametric vectors/matrices

Input:
The reference trajectories: $\{x_r, \dot{x}_r\}_{m=1,t=1}^{M,T}$;
The desired force profiles: $\{F_d\}_{m=1,t=1}^{M,T}$;
The constant matrices/coefficients: Q_S, Q_D,Q_F,Q_r, β, α.
Output:
The parametric vectors/matrices: θ_{K_S}, θ_{K_D}, θ_F.

begin
  Create a parametric skill database ;
  Initialize the parameters θ_{K_S}, θ_{K_D}, and θ_F;
  for $t = 1$ *to* T **do**
    Get the robot current states;
    Compute the sliding error using (5);
    Compute the adaptation of reference trajectory with (18);
    for $m = 1$ *to* M **do**
      Compute $\Omega_1(t)$, $\Omega_2(t)$, and $\Omega_3(t)$;
      for $n = 1$ *to* N **do**
        for $j = 1$ *to* N *AND* $j \neq n$ **do**
          Compute $\sum_{j=1}^{N} \theta_{K_s,m,j}(t) g_j$, $\sum_{j=1}^{N} \theta_{K_D,m,j}(t) g_j$, $\sum_{j=1}^{N} \theta_{F,m,j}(t) g_j$;
        end
        Update the parametric matrix $\theta_{K_S}(t+1)$, $\theta_{K_D}(t+1)$, and $\theta_F(t+1)$;
      end
    end
    Add the learned parametric vectors/matrices to the skill database; Generate force/torque control commands;
    Send commands to robot actuators;
  end
end

with

$$\Omega_2(t) = Q_{D,m}\varepsilon_m(t)\dot{x}_m(t) + (1 - Q_{D,m}\beta)\theta_{K_D,m}^T(t)g \quad (38)$$

And

$$\theta_{F,m,n}(t+1) = \frac{\Omega_3(t) - \sum_{j=1}^{N} \theta_{F,m,j,j\neq n}(t) g_{j,j\neq n}}{1 - \sum_{j=1}^{N} g_{j,j\neq n}} \quad (39)$$

with

$$\Omega_3(t) = Q_{F,m}\varepsilon_m(t) + (1 - Q_{F,m}\beta)\theta_{F,m}^T(t)g + Q_{F,m}Q_{r,m}\Delta\varepsilon_r(t) \quad (40)$$

The derivation of the updating laws for θ_{K_S}, θ_{K_D} and θ_{K_F} is given in Appendix. The learning of impedance and feedforward force parametric vectors in an online manner is summarized in Algorithm 1.

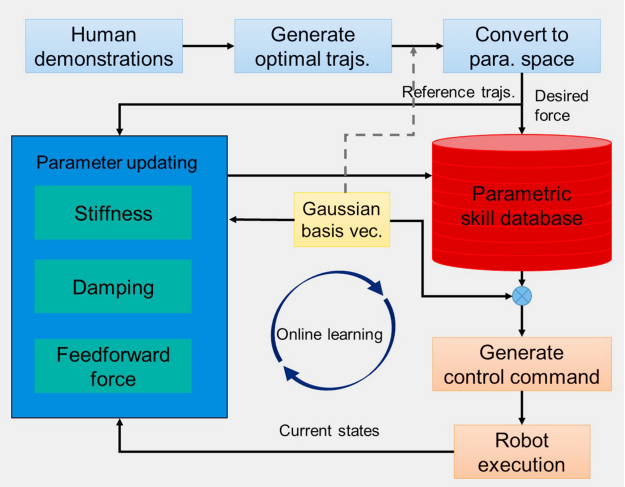

Fig. 1: The diagram of integrating learning of a compliant skill in the parametric space.

D. *Integrating learning/representation of a compliant skill in the parametric space*

Our approach requires two phases for integrating learning/representation of a compliant skill in the parametric space. In the first phase, the goal is to obtain the parametric vectors θ_p and θ_{F_d}. The human/robot states including position trajectories and interaction forces during human demonstrations are first recorded as the observation data. After human demonstrations and generation of optimal trajectories, the position trajectories and desired force profiles are converted to the corresponding parametric vectors (matrices for multiple DOFs) and stored in the parametric skill database. This phase is completed offline before the robotic execution.

The second phase aims to address the learning of the other parameters, i.e., θ_{K_S}, θ_{K_D}, and θ_F during the robotic execution of the task. These parameters are first initialized by setting the elements as constant values. During a control loop, these parametric vectors/matrices and the Gaussian basis are performed inner product to yield the control variables and further generate the control command. At each time step, the parameters of the stiffness, damping, and feedforward force are adapted online with the robot current states, the reference position trajectories, and the desired force profiles which are obtained in the first phase. Meanwhile, the learned parameters are also added to the parametric skill database. The procedure of the skill learning process is illustrated in Fig. 1.

E. *Comments*

1) Learning/control in joint space: Although the learning and control procedure is written in the Cartesian space, our approach can also be easily implemented in the joint space. In that case, the robot states including joint angles and the interaction forces with the external environments are recorded during demonstrations. The desired joint torques are obtained through the inverse kinematics with the forces collected during demonstrations. Then, the learning/control procedure is the same as described above.

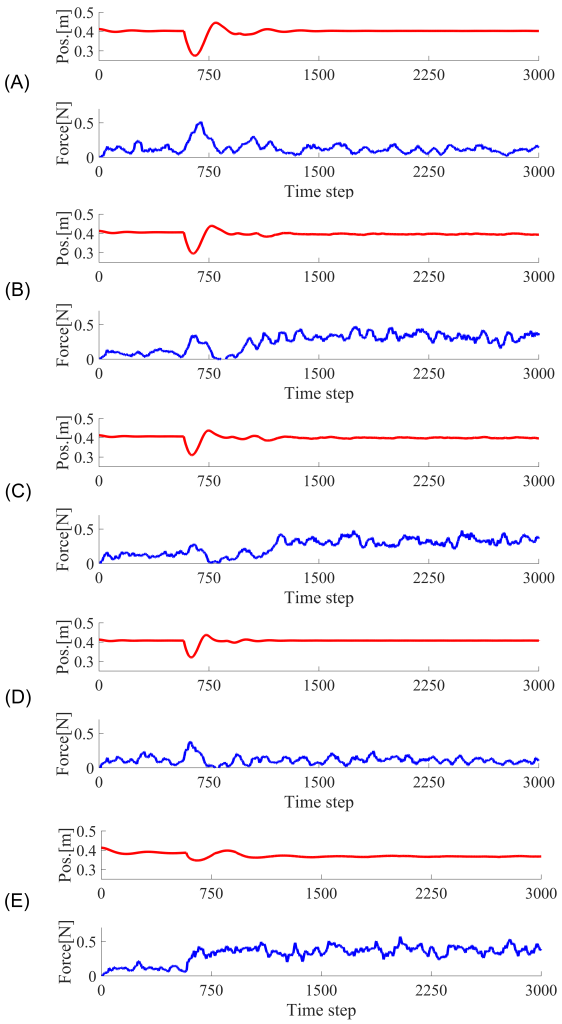

Fig. 2: The collected robot endpoint position and force profiles in z axis under conditions (A)-(E).

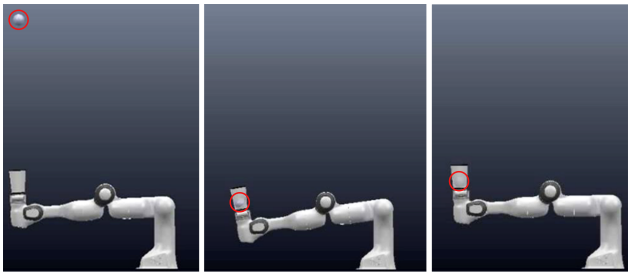

Fig. 3: Simulation of the catching-a-ball task. From left to right: before contact, during contact and after contact.

2) Stability and parameters convergence: It is noted that although our approach enables the learning of stiffness, damping, and feedforward force in the parametric space, the control variables are formed in the trajectory-level (see Fig. 1) before the generation of the control commands. The stability issue and parameters convergence of the controller can be analyzed and guaranteed using the same procedure in [27, 28].

TABLE I: The results of the catching-a-ball task.

	(A)	(B)	(C)	(D)	(E)
Succeed?	NO	YES	YES	NO	YES
Rebound?	YES	YES	YES	YES	NO
RMSE [m]	0.0224	0.0177	0.0146	0.0141	0.0298

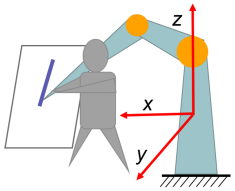

Fig. 4: The illustration of the experimental setup for the drawing-a-line task.

V. Experimental Validation

A. *Catching-a-ball task in simulation*

A catching-a-ball task in the simulation environment PyRep [33] is considered to validate the proposed control strategy. The experimental setting is that a Franka Panda robot arm is controlled in the torque control mode with a fixed pose to catch a ball falling from the height of 1.6 [m]. The angles of the seven joints of the robot arm are set as $[0, -90, 0, 0, 0, 90, 45]$. Bullet 2.78 is chosen as the simulation engine with the time step 1.0 [ms].

We compare our approach with the conventional fixed impedance control. The stiffness matrix for the 7 DOFs is set as $\varsigma \times diag\{100, 100, 100, 100, 100, 50, 50\}$, where ς is a constant coefficient. The task is performed under five conditions: (A) $\varsigma = 15$, (B) $\varsigma = 20$, (C) $\varsigma = 25$, (D) $\varsigma = 30$, and (E) using the proposed control strategy with $Q_K = 300$, $Q_D = 50$, $Q_F = 5$, $Q_R = 0$, $\beta = 0.01$, and $\alpha = 50$[1]. Three factors are considered to evaluate the performances: 1) *Whether the ball is caught successfully?* 2) *Whether the ball is rebounded back after contact?* 3) Root Mean Square Error (RMSE) values of the positions in z axis.

The experimental results are summarized in Table I, and Fig. 2 shows the measured position and force profiles in z axis. All the force values are filtered with the window size 50. We observe that under the conditions (A) and (D) the robot is not able to catch the ball successfully, which is visualized from the force profiles in Fig. 2 (B) and (C): the contact force is almost zero from 800th time step. It suggests too low or too high stiffness both result in task failure under the fixed impedance control mode. Under conditions (B), (C), and (E), the task is successfully completed (see Fig. 3 for an example). It is observed that, however, under the fixed impedance mode the ball tends to be rebounded back after contact, due to the rigid contact between the ball and the cup. This is visualized from the force profiles in Fig. 2 (B) and (C): from 600th to 800th time steps the contact force values decrease to zero. Using the proposed approach the contact force gradually increases to a nearly constant value after contact, which means a compliant catching process is achieved, see Fig. 2 (E). The RMSE values

[1]We set the same values for all DOFs in the experiments.

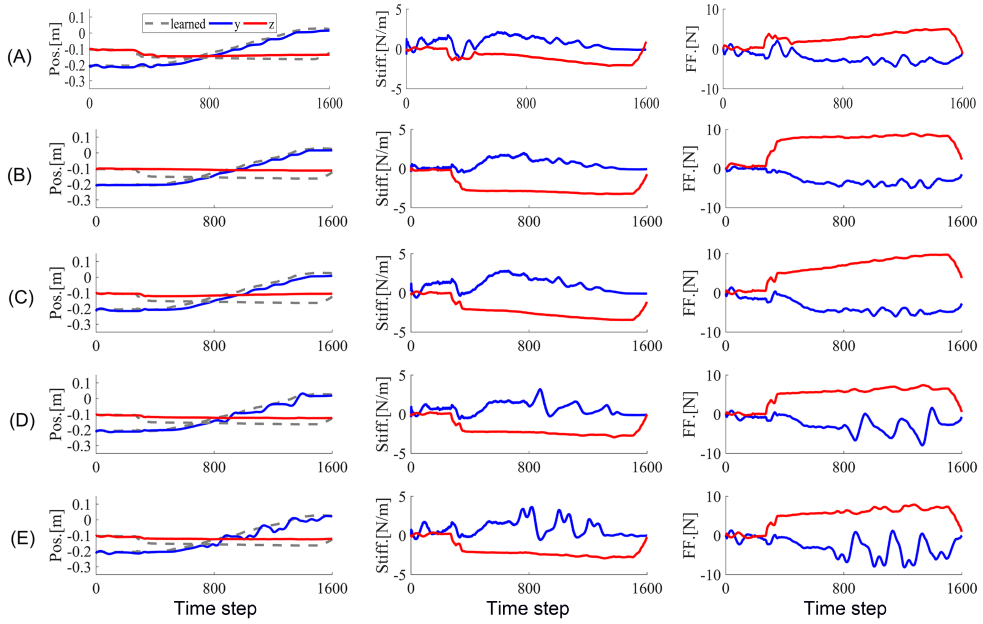

Fig. 5: Left column: the learned position trajectories from demonstrations (gray dashed lines) and the collected position trajectories (colored lines) during task reproductions. The middle and right columns are the learned stiffness and feedforward force profiles during task reproductions. The subplots (A)-(E) correspond to the five different conditions successively.

TABLE II: The RMSE values for the drawing-a-line task of the measured endpoint positions with respect to the demonstrations.

RMSE [m]	(A)	(B)	(C)	(D)	(E)
x	0.0108	0.0041	0.0077	0.0066	0.0093
y	0.0154	0.0135	0.0198	0.0167	0.0207
z	0.0161	0.0433	0.040	0.0314	0.0312

suggest the fixed impedance control has a better performance in position tracking. Our approach sacrifices the position tracking accuracy to maintain the compliant behaviours.

B. *Drawing-a-line task*

A drawing-a-line task is first performed to verify the adaptability of the proposed approach. A Sawyer robot is taught by a human tutor to draw a straight line along the y axis in the $x-y$ plane (see Fig. 4). A whiteboard pen is attached to the endpoint of the robot as a tool for drawing. During the demonstration phase, the tutor holds on the endpoint to drive the robot which is controlled in the *demonstration mode* to complete the task, and the endpoint motion trajectories, as well as force profiles, are recorded. For the robot production of the task after the human demonstration, we set five different conditions as follows:

Condition (A): The robot reproduces the drawing task in the same task scenario as in the demonstration phase, i.e., without any change of the settings.

Condition (B): We change the task setting by moving up the whiteboard about 5cm in z direction.

Condition (C): Based on condition (B), the whiteboard is further rotated about 10° along x axis.

Condition (D): A small disturbance is applied to the robot by slightly pushing the endpoint along the y axis.

Condition (E): Compared with condition (D), a relatively larger disturbance is applied to the robot that would cause slightly unstable interactions.

The main parameters are set as below: $Q_K = 40$, $Q_D = 2$, $Q_F = 4$, $Q_R = 0.05$, $\beta = 0.05$, and $\alpha = 30$, and the number of Gaussian components N is set 15. The learning results of this task are shown in Fig. 5. The first row shows the collected position trajectories in the demonstration and reproductions in y and z directions, respectively. The second and third rows are the learned stiffness and feedforward force profiles in these reproductions under different conditions, corresponding to the subplots (A)-(E). Under the first condition, the robot can reproduce the drawing task successfully by slightly adapting the stiffness and feedforward force profiles, to make the robot endpoint to follow the reference trajectories in the absence of the human guidance. When the whiteboard is raised in z direction, it is observed that both stiffness and feedforward force in the z axis would increase to adapt to this change. However, these profiles in y direction almost remain the same, which means the profiles are adapted selectively to respond to the task dynamics. This adaptability can also be further observed under the third task condition [see Fig. 5(C)]. When the whiteboard is rotated, our approach could *recognize* this change and respond to it by correspondingly adapting the stiffness and feedforward force profiles in z axis, and keep the stiffness and force almost unaffected in the y axis. The ability of resistance to external disturbances is tested in the last two conditions. A small disturbance is first applied to the robot in y direction, and we can see that our approach could respond to the disturbance to reduce the position error by mostly adapting the feedforward force, but the stiffness does not change too

Fig. 6: The experimental setup for the writing task during the demonstration phase.

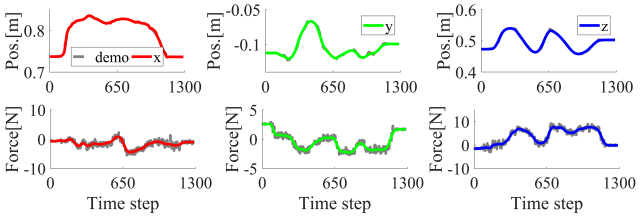

Fig. 7: An example of the learned position and force profiles (colored lines) with respect to the demonstrations (gray lines).

much [see Fig. 5(D)]. If a larger disturbance is applied to the robot that might cause unstable interaction, however, both stiffness and feedforward force profiles could be adapted to reduce the influence of the disturbance [see Fig. 5(E)]. This observation is consistent with the principles of human motor learning and the experimental findings in [27].

Table II shows the RMSE values for the drawing-a-line task of the measured endpoint positions with respect to the demonstrations. The RMSE values in different task conditions can verify the above analysis. For instance, the RMSE values in the y axis in the first two conditions are close, and the RMSE values in the z axis in the last two conditions are close. It means that the different settings in one axis would not largely affect the situation in another axis.

C. *Writing-letters task*

Another task, i.e., writing task, is then performed to further verify the proposed approach. The experimental setup for the task demonstration is shown in Fig. 6. It shows how a human tutor teaches the robot writing on a whiteboard in the $x-z$ plane. It should be noted that the human tutor only drags the endpoint of the robot during the demonstration, and no external force is applied to the other parts of the robot arm. First, the human tutor teaches the robot to write a character, the robot then reproduces the writing of this character with the online learning of impedance and feedforward force profiles, along with the execution of the position trajectories. To add uncertainties and increase the difficulty of this task, the whiteboard is not completely fixed onto the ground in x axis, and can also be rotated along the y axis.

Different types of characters are written in this task. The human tutor teaches the robot to write two Chinese characters, 'shi' and 'ba', two English letters, 'b' and 'w', and two numbers, '2' and '8'. The robot then autonomously writes these characters by itself. Fig. 7 shows an example of the learned position trajectories and force profiles with respect to the demonstration ones. As shown in Fig. 8, the task can be reproduced by the robot successfully with the proposed approach. Some defects can also be seen in the reproductions which may be due to the uncertainties. The collected position trajectories and the learned stiffness and feedforward force profiles are illustrated in Fig. 9. Table III shows the RMSE values for the writing task of the measured endpoint positions with respect to the demonstration ones.

The stiffness and feedforward force profiles are both adapted simultaneously during the writing process as observed in the last task. Due to the uncertainties in x direction, the position tracking errors in x axis are relatively larger than that in y and z directions (see Table III). In order to overcome the uncertainties, however, the stiffness profiles in the x axis are adapted to a larger degree than that in the z axis, as can be seen in Fig. 9. This adaptability of our approach can automatically enable the rigid control in one axis but remain compliant in another one so that the robot could flexibly perform the task. It is interesting to find that the shapes of the stiffness and feedforward force profiles can sometimes demonstrate the features of the strokes, especially for the writing of the Chinese characters. For instance, the feedforward force in the x axis for the horizontal and vertical strokes in the character 'shi' is almost kept constant, while for the left-falling and right-falling strokes in the character 'ba' it is first slowly increased and then decreased. This adaptation is similar to the adaptation of human arm stiffness/force during the process of writing these strokes. We also find that the reproduction of the English and number characters are more difficult for the robot. This may be explained by the fact that the English and number characters consist of continuous strokes. The robot has to interact with the environment continuously and the cumulative errors in former steps may have an influence on the execution in later steps.

TABLE III: The RMSE values for the writing experiment of the measured endpoint positions with respect to the demonstrations.

RMSE [m]	(A)	(B)	(C)	(D)	(E)	(F)
x	0.0323	0.0420	0.0565	0.0413	0.0315	0.0238
y	0.0156	0.0242	0.0295	0.0134	0.0156	0.0242
z	0.0093	0.0234	0.0271	0.0161	0.0103	0.0140

Robot learning of writing skills has been discussed in several works in the last several years, and shown fine performances if using a brush that can avoid hard physical interaction between the robot and the environment (see e.g., [34, 35]). Our experiment focuses on allowing the robot to learn the contact-rich handwriting skills by adapting to the physical interaction with its environments, thanks to the stiffness/force adaptation mechanism. Compared with the writing skill learning method in [36], the proposed approach enables the efficient online learning of stiffness and force profiles during reproduction and does not require a time-consuming process of measurement of human arm stiffness in advance before the demonstration.

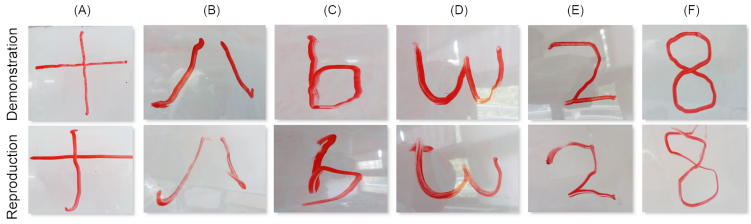

Fig. 8: The human demonstrations (upper row) and robot reproductions (bottom row) of the characters. From (A) to (F): the Chinese characters ‘shi’ and ‘ba’, the English letters ‘b’ and ‘w’, and the numbers ‘2’ and ‘8’.

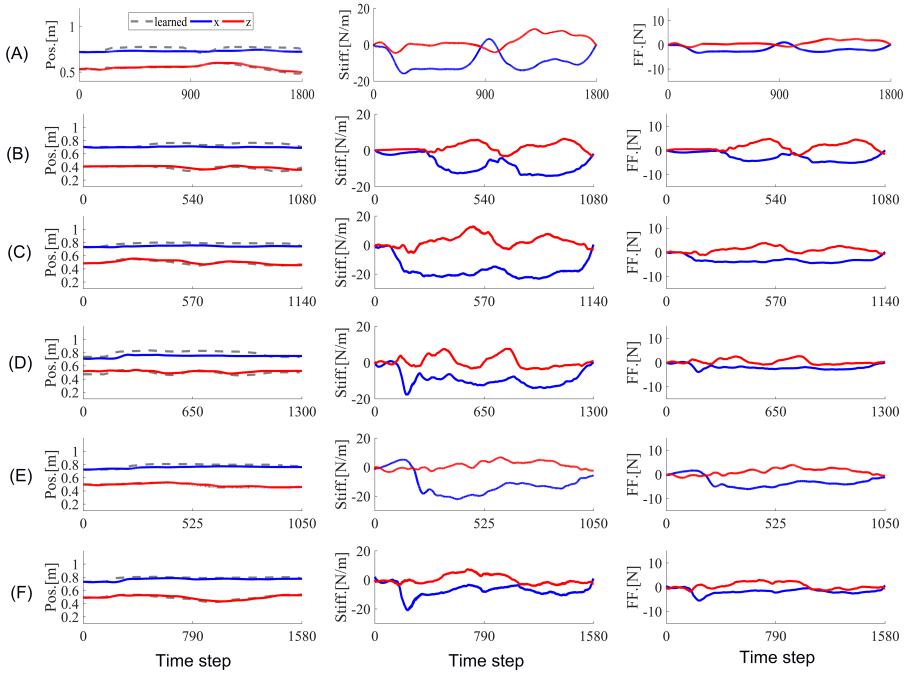

Fig. 9: Left column: the learned position trajectories from demonstrations (gray dashed lines) the collected position trajectories (colored lines) during task reproductions. The middle and right columns are the learned stiffness and feedforward force profiles during task reproductions.

VI. Conclusion and Future Work

We develop a novel learning and control framework that allows the robots to learn compliant manipulation skills from human demonstrations, taking into consideration of both motion data and force information. We have successfully verified our approach in three scenarios including one simulation and two real-world tasks and on two different robotic manipulators. The proposed representation enables to encode a skill by a set of parameters that can represent the compliant profiles including motion trajectories, impedance, and force profiles. Furthermore, the compliant profiles can be directly updated in the parametric space instead of the trajectory level, which may facilitate robotic skill learning and transfer.

Our approach is derived from the computational model of the control strategy of human motor learning. As a result, the impedance and feedforward force profiles could be adapted simultaneously in an online manner during task reproduction, to deal with external uncertainties. Our bio-inspired approach integrates learning and control to achieve the skill transfer from the human tutor to the robot.

Our approach has several weaknesses: i) it does not guarantee accurate trajectory tracking. Therefore, our approach is more suitable for task scenarios where compliant manipulation instead of a high position accuracy is required; ii) it requires manually setting the open parameters that may vary from one task to another. Our strategy is to safely start with relatively low values, and then increase them progressively; and iii) Our approach has shown its generalizability, however, it is still limited in varying task scenarios. For instance, once the compliant profiles are learned, they may not be able to deal with a significantly different task scenario.

One future research line is to enable efficient skill generalization based on our approach. This may be achieved by directly generalizing the parameters using statistical learning algorithms such as Gaussian process regression (GPR) associated with task-specific variables and external perception information, in order to adapt these compliant profiles to deal with new task situations. The generalization process might be similar to [37]. Another future work is to enable encoding of orientation data (e.g., quaternions and rotational stiffness

profiles) in the Cartesian space, making the approach suitable for more task scenarios.

APPENDIX

According to the updating law in (11), for the m-th DOF at the time step t, we have

$$\Delta K_S, m(t) = Q_{S,m}[\varepsilon_m(t)x_m(t) - \beta K_{S,m}(t)] \tag{41}$$

Then, we have

$$\Delta\theta^T_{K_S,m}(t)g = Q_{S,m}[\varepsilon_m(t)x_m(t) - \beta\theta^T_{K_S,m}(t)g] \tag{42}$$

$$\Delta\theta^T_{K_S,m}(t) = \theta^T_{K_S,m}(t+1) - \theta^T_{K_S,m}(t) \tag{43}$$

Combining the above two equations, we have

$$\begin{aligned}\theta^T_{K_S,m}(t+1)g = {} & Q_{S,m}\varepsilon_m(t)x_m(t) \\ & + (1 - Q_{S,m}\beta)\theta^T_{K_S,m}(t)g\end{aligned} \tag{44}$$

The right hand side of the above equation is denoted as $A(t)$. For simplicity, we neglect the subscript, superscript and timestamps from now on. The above equation is written as

$$\Omega_1 = \theta^T g = \theta_1 g_1 + ... + \theta_n g_n + ... + \theta_N g_N \tag{45}$$

Note that g_n will satisfy the constraints as below.

$$0 < g_n < 1, \quad \sum_{n=1}^{N} g_n = 1 \tag{46}$$

Then, we can obtain

$$\Omega_1 = \theta_1 g_1 ... + \theta_n(1 - \sum_{j=1}^{N} g_{j,j\neq n}) + ... + \theta_N g_N \tag{47}$$

Then, we have

$$\theta_n(1 - \sum_{j=1}^{N} g_{j,j\neq n}) = \Omega_1 - \sum_{j=1}^{N} \theta_{j,j\neq n} g_{j,j\neq n} \tag{48}$$

Finally, we have

$$\theta_n = \frac{\Omega_1 - \sum\limits_{j=1}^{N} \theta_{j,j\neq n} g_{j,j\neq n}}{1 - \sum\limits_{j=1}^{N} g_{j,j\neq n}} \tag{49}$$

The derivation of the updating laws for the damping θ_{K_D} and the feedforward θ_F can be achieved in a similar way. We neglect the denominator parts in practical applications.

REFERENCES

[1] H. Ravichandar, A. S. Polydoros, S. Chernova, and A. Billard, "Recent advances in robot learning from demonstration," *Annual Review of Control, Robotics, and Autonomous Systems*, vol. 3, 2020.

[2] Z. Zhu and H. Hu, "Robot learning from demonstration in robotic assembly: A survey," *Robotics*, vol. 7, no. 2, p. 17, 2018.

[3] W. Xu, J. Chen, H. Y. Lau, and H. Ren, "Automate surgical tasks for a flexible serpentine manipulator via learning actuation space trajectory from demonstration," in *2016 IEEE International Conference on Robotics and Automation (ICRA)*. IEEE, 2016, pp. 4406–4413.

[4] X. Zhang, J. Zhang, and J. Zhong, "Toward navigation ability for autonomous mobile robots with learning from demonstration paradigm: A view of hierarchical temporal memory," *International Journal of Advanced Robotic Systems*, vol. 15, no. 3, p. 1729881418777939, 2018.

[5] J. Duan, Y. Gan, M. Chen, and X. Dai, "Adaptive variable impedance control for dynamic contact force tracking in uncertain environment," *Robotics and Autonomous Systems*, vol. 102, pp. 54–65, 2018.

[6] F. J. Abu-Dakka, L. Rozo, and D. G. Caldwell, "Force-based variable impedance learning for robotic manipulation," *Robotics and Autonomous Systems*, vol. 109, pp. 156–167, 2018.

[7] C. Zeng, C. Yang, H. Cheng, Y. Li, and S.-L. Dai, "Simultaneously encoding movement and semg-based stiffness for robotic skill learning," *IEEE Transactions on Industrial Informatics*, vol. 17, no. 2, pp. 1244–1252, 2020.

[8] X. Yu, W. He, Y. Li, C. Xue, J. Li, J. Zou, and C. Yang, "Bayesian estimation of human impedance and motion intention for human-robot collaboration," *IEEE Transactions on Cybernetics*, 2019.

[9] W. He, C. Xue, X. Yu, Z. Li, and C. Yang, "Admittance-based controller design for physical human-robot interaction in the constrained task space," *IEEE Transactions on Automation Science and Engineering*, 2020.

[10] L. Fraser, B. Rekabdar, M. Nicolescu, M. Nicolescu, D. Feil-Seifer, and G. Bebis, "A compact task representation for hierarchical robot control," in *2016 IEEE-RAS 16th International Conference on Humanoid Robots (Humanoids)*. IEEE, 2016, pp. 697–704.

[11] A. J. Ijspeert, J. Nakanishi, and S. Schaal, "Movement imitation with nonlinear dynamical systems in humanoid robots," in *Proceedings 2002 IEEE International Conference on Robotics and Automation*, vol. 2. IEEE, 2002, pp. 1398–1403.

[12] W. He and Y. Dong, "Adaptive fuzzy neural network control for a constrained robot using impedance learning," *IEEE transactions on neural networks and learning systems*, vol. 29, no. 4, pp. 1174–1186, 2017.

[13] Y. Dong and B. Ren, "Ude-based variable impedance control of uncertain robot systems," *IEEE Transactions on Systems, Man, and Cybernetics: Systems*, vol. 49, no. 12, pp. 2487–2498, 2019.

[14] T. Sun, L. Peng, L. Cheng, Z.-G. Hou, and Y. Pan, "Stability-guaranteed variable impedance control of robots based on approximate dynamic inversion," *IEEE Transactions on Systems, Man, and Cybernetics: Systems*, 2019.

[15] C. Zeng, X. Chen, N. Wang, and C. Yang, "Learning compliant robotic movements based on biomimetic motor adaptation," *Robotics and Autonomous Systems*, vol. 135, p. 103668, 2021.

[16] J. Buchli, F. Stulp, E. Theodorou, and S. Schaal, "Learning variable impedance control," *The International Journal of Robotics Research*, vol. 30, no. 7, pp. 820–833, 2011.

[17] J. Luo, E. Solowjow, C. Wen, J. A. Ojea, A. M. Agogino, A. Tamar, and P. Abbeel, "Reinforcement learning on variable impedance controller for high-precision robotic assembly," in *2019 International Conference on Robotics and Automation (ICRA)*. IEEE, 2019, pp. 3080–3087.

[18] M. Bogdanovic, M. Khadiv, and L. Righetti, "Learning variable impedance control for contact sensitive tasks," *IEEE Robotics and Automation Letters*, vol. 5, no. 4, pp. 6129–6136, 2020.

[19] C. Yang, C. Zeng, C. Fang, W. He, and Z. Li, "A dmps-based framework for robot learning and generalization of humanlike variable impedance skills," *IEEE/ASME Transactions on Mechatronics*, vol. 23, no. 3, pp. 1193–1203, 2018.

[20] F. Bian, D. Ren, R. Li, P. Liang, K. Wang, and L. Zhao, "An extended dmp framework for robot learning and improving variable stiffness manipulation," *Assembly Automation*, vol. 40, no. 1, pp. 85–94, 2019.

[21] A. Naceri, T. Schumacher, Q. Li, S. Calinon, and H. Ritter, "Learning optimal impedance control during complex 3d arm movements," *IEEE Robotics and Automation Letters*, vol. 6, no. 2, pp. 1248–1255, 2021.

[22] M. Deniša, A. Gams, A. Ude, and T. Petrič, "Learning compliant movement primitives through demonstration and statistical generalization," *IEEE/ASME transactions on mechatronics*, vol. 21, no. 5, pp. 2581–2594, 2015.

[23] L. Rozo Castañeda, S. Calinon, D. Caldwell, P. Jimenez Schlegl, and C. Torras, "Learning collaborative impedance-based robot behaviors," in *Proceedings of the twenty-seventh AAAI conference on artificial intelligence*, 2013, pp. 1422–1428.

[24] Z. Li, C. Xu, Q. Wei, C. Shi, and C.-Y. Su, "Human-inspired control of dual-arm exoskeleton robots with force and impedance adaptation," *IEEE Transactions on Systems, Man, and Cybernetics: Systems*, 2018.

[25] G. Ganesh, A. Albu-Schäffer, M. Haruno, M. Kawato, and E. Burdet, "Biomimetic motor behavior for simultaneous adaptation of force, impedance and trajectory in interaction tasks," in *2010 IEEE International Conference on Robotics and Automation*. IEEE, 2010, pp. 2705–2711.

[26] E. Burdet, G. Ganesh, C. Yang, and A. Albu-Schäffer, "Interaction force, impedance and trajectory adaptation: by humans, for robots," in

Experimental Robotics. Springer, 2014, pp. 331–345.
[27] C. Yang, G. Ganesh, S. Haddadin, S. Parusel, A. Albu-Schaeffer, and E. Burdet, "Human-like adaptation of force and impedance in stable and unstable interactions," *IEEE transactions on Robotics*, vol. 27, no. 5, pp. 918–930, 2011.
[28] Y. Li, G. Ganesh, N. Jarrassé, S. Haddadin, A. Albu-Schaeffer, and E. Burdet, "Force, impedance, and trajectory learning for contact tooling and haptic identification," *IEEE Transactions on Robotics*, vol. 34, no. 5, pp. 1170–1182, 2018.
[29] C. Zeng, H. Su, Y. Li, J. Guo, and C. Yang, "An approach for robotic leaning inspired by biomimetic adaptive control," *IEEE Transactions on Industrial Informatics*, 2021.
[30] K. P. Tee, D. W. Franklin, M. Kawato, T. E. Milner, and E. Burdet, "Concurrent adaptation of force and impedance in the redundant muscle system," *Biological cybernetics*, vol. 102, no. 1, pp. 31–44, 2010.
[31] V. S. Chib, J. L. Patton, K. M. Lynch, and F. A. Mussa-Ivaldi, "Haptic identification of surfaces as fields of force," *Journal of neurophysiology*, vol. 95, no. 2, pp. 1068–1077, 2006.
[32] A. J. Ijspeert, J. Nakanishi, and S. Schaal, "Trajectory formation for imitation with nonlinear dynamical systems," in *Proceedings 2001 IEEE/RSJ International Conference on Intelligent Robots and Systems. Expanding the Societal Role of Robotics in the the Next Millennium (Cat. No. 01CH37180)*, vol. 2. IEEE, 2001, pp. 752–757.
[33] S. James, M. Freese, and A. J. Davison, "Pyrep: Bringing v-rep to deep robot learning," *arXiv preprint arXiv:1906.11176*, 2019.
[34] Y. Sun, H. Qian, and Y. Xu, "Robot learns chinese calligraphy from demonstrations," in *2014 IEEE/RSJ International Conference on Intelligent Robots and Systems*. IEEE, 2014, pp. 4408–4413.
[35] F. Chao, Y. Huang, C.-M. Lin, L. Yang, H. Hu, and C. Zhou, "Use of automatic chinese character decomposition and human gestures for chinese calligraphy robots," *IEEE Transactions on Human-Machine Systems*, vol. 49, no. 1, pp. 47–58, 2018.
[36] P. Liang, C. Yang, Z. Li, and R. Li, "Writing skills transfer from human to robot using stiffness extracted from semg," in *2015 IEEE international conference on cyber technology in automation, control, and intelligent systems (CYBER)*. IEEE, 2015, pp. 19–24.
[37] T. Petrič, A. Gams, L. Colasanto, A. J. Ijspeert, and A. Ude, "Accelerated sensorimotor learning of compliant movement primitives," *IEEE Transactions on Robotics*, vol. 34, no. 6, pp. 1636–1642, 2018.

Chao Zeng (S'18-M'20) received the Ph.D. degree in pattern recognition and intelligent systems from South China University of Technology, Guangzhou, China, in December 2019. He visited Department of Informatics, Universitt Hamburg(UHH), Germany, from October 2018 to October 2019. He is a research assistant in Guangdong University of Technology where he did this research from January 2020. He is a research associate at UHH from September 2020. His research interest includes robot learning and control, physical human-robot interaction.

Yanan Li (S'10-M'14) received the BEng and MEng degrees from the Harbin Institute of Technology, China, in 2006 and 2008, respectively, and the PhD degree from the National University of Singapore, in 2013. Currently he is a Lecturer in Control Engineering with the Department of Engineering and Design, University of Sussex, UK. His general research interests include human-robot interaction, robot control and control theory and applications.

Jing Guo obtained his Ph.D degree from LIRMM, CNRS-University of Montpelier, France in 2016. He received his master and bachelor degree from Guangdong University of Technology in 2009 and 2012 respectively. He has been research fellow at National University of Singapore (NUS) during 2016-2018. He is an associate proferssor affilicated with Guangdong University of Technology. His current research interests include robotic control and learning, haptic bilateral teleoperation, and surgical robotics, has served as guest editor for IEEE RA-L, Frontiers in Robotics and AI, etc.

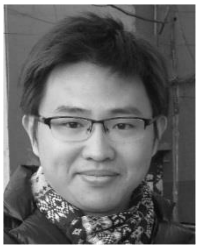

Zhifeng Huang received his BEng degree in Mechatronics Engineering from the South China University of Technology, China, in 2007, and his MEng degree in the same discipline from the Harbin Institute of Technology, China, in 2010. In 2014, he received his PhD from the Department of Precision Engineering, the University of Tokyo. He is now a associate professor at the School of Automation, Guangdong University of Technology, China. His research interests include humanoid robot, nursing engineering, skill acquisition, and healthcare robotics.

Ning Wang is a Senior Lecturer in Robotics at the Bristol Robotics Laboratory, University of the West of England, United Kingdom. She received the M.Phil. and Ph.D. degrees in electronics engineering from the Department of Electronics Engineering, The Chinese University of Hong Kong, Hong Kong, in 2007 and 2011, respectively. Ning has rich project experience, she has been key member of EU F-P7 Project ROBOT-ERA, EU Regional Development Funded Project ASTUTE 2020 and industrial projects with UK companies. She has been awarded several awards including best paper award of ICIRA'15, best student paper award nomination of ISCSLP'10, and award of merit of 2008 IEEE Signal Processing Postgraduate Forum, etc. Her research interests lie in signal processing, intelligent data analysis, human-robot interaction and autonomous driving.

Chenguang Yang henguangYanghenguangYangC (M'10-SM'16) received the Ph.D. degree in control engineering from the National University of Singapore, Singapore, in 2010, and postdoctoral training in human robotics from the Imperial College London, London, U.K. He was awarded UK EPSRC UKRI Innovation Fellowship and individual EU Marie Curie International Incoming Fellowship. As lead author, he won the IEEE Transactions on Robotics Best Paper Award (2012) and IEEE Transactions on Neural Networks and Learning Systems Outstanding Paper Award (2022).He is a Co-Chair of IEEE Technical Committee on Collaborative Automation for Flexible Manufacturing (CAFM) and a Co-Chair of IEEE Technical Committee on Bio-mechatronics and Bio-robotics Systems (B2S). He serves as Associate Editors of a number of international top journals including Neurocomputing and seven IEEE Transactions.His research interest lies in human robot interaction and intelligent system design.